Publ. Obs. Astron. Belgrade No. 50 (1995), 21 – 26 *Invited lecture*

ON INVERSE METHODS USED AT BELGRADE OBSERVATORY FOR ANALYSIS OF SPECTRAL LINE SHAPES

I. VINCE, L. Č. POPOVIĆ, S. JANKOV, G. DJURAŠEVIĆ,
O. ATANACKOVIĆ-VUKMANOVIĆ and D. JEVREMOVIĆ
Astronomical Observatory, Volgina 7, 11050 Belgrade, Yugoslavia
E-mail ivince@aob.aob.bg.ac.yu

Abstract. In this paper we present inverse methods used for analysis of the spectral line shapes at Belgrade Observatory. A short description of the methods and some examples of application are given.

1. INTRODUCTION

Spectral line profiles of stars and other celestial objects, and those of laboratory sources may have a very complex shape caused by emission and absorption of different parts of the source. For instance, stellar spectral line profiles may consist of intrinsic component and of a component, which is formed in the circumstellar or/and interstellar space. The intrinsic component might be perturbed by surface features (e.g., dark spots, bright spots, chemical inhomogeneities etc.).

To study the physics of these parts separately it is necessary to reconstruct their original spectral line shapes. This, in principle, can be done by using the direct or the inverse method. At our Observatory we have developed inverse methods for the reconstruction of intrinsic and interstellar spectral line profiles of cool late-type stars, for Doppler imaging of a stellar surface and for reconstruction of spectral line shapes of different surrounding regions of quasars and Seyfert galaxies.

2. THE PRINCIPLES OF INVERSE METHODS

Let us suppose that the observed profile can be presented by a model through a function $f(x, a_1, a_2, ..., a_n)$, where $a_1, a_2, ..., a_n$ are the known but undetermined parameters of the model, which depend on physical conditions in the observed object. The inverse method consists of determining these parameters so that the difference between the observed and the calculated data reaches its minimum value.

3. STELLAR LINES

3. 1. STELLAR SPECTRAL LINES WITH INTERSTELLAR ABSORPTION

When the observed stellar spectral lines show interstellar absorption, for a separation of the intrinsic line profile from the interstellar one we can use the following procedure.

We suppose that a cloud of interstellar media exists between our telescope and the observed star, and that $I^0(\lambda)$ is the intrinsic intensity of the stellar line. Then for the observed intensity $I(\lambda)$ we could write the following equation

$$I(\lambda) = I^0(\lambda)e^{-\Delta\tau_\lambda} + \int_1^2 S(t)e^{-(\tau_\lambda - t_\lambda)}dt_\lambda, \tag{1}$$

where $S(t)$ is the source function of the absorption interstellar media and τ is the optical depth. If we suppose that in the interstellar cloud there are no emission sources, i.e., $S(t) = 0$, and $\Delta\tau << 1$, equation (1) may be rewritten as

$$I(\lambda) = I^0(\lambda)(1 - \Delta\tau). \tag{2}$$

For $\Delta\tau$ we may take

$$\Delta\tau = \overline{\varphi} \cdot T,$$

where T is the optical depth of the cloud at the core of line prcfile. If we take that $\overline{\varphi}T$ is a Gaussian function, then for observed intensity distribution of a line we may write

$$I(\lambda) = I^0(\lambda)(1 - a_1 e^{-((x-a_2)/a_3)^2}). \tag{3}$$

From eq. (3) we may reconstruct the intrinsic stellar line profile $I^0\lambda$ and the interstellar absorption line profile by determining the free parameters (a_i; $i = 1, 2, 3$) using the inverse method technique.

As an example of the inverse method technique the reconstruction of a high-resolution IUE spectrum of the RS CVn type star HR 7275 is presented. The observed MgII h spectral line profile shows a prominent interstellar absorption component near the core of the emission line profile. In Fig. 1 are shown the observed and the reconstructed intrinsic MgII h spectral line profile with the best fit parameters.

3. 2. IMAGE RECONSTRUCTION OF LATE-TYPE STARS FROM SPECTROSCOPIC ROTATIONAL MODULATION

A Doppler imaging method consists of using the effect of localized spots on line profiles, Doppler broadened due to the star's rotation. This method can be used to derive an image of photospheric and chromospheric features (spots and plages).

The image reconstruction can be performed using a set of the observed line profiles, which covers the star's rotation period well. This set of line profiles creates the data vector. Doppler imaging can be applied to fast rotating stars only.

Using the term image to represent the distribution of the specific intensities on the surface of the star under investigation it was shown (Jankov, 1992) that the image is related in some known way to the spectroscopic data. In addition it is showed (Jankov and Foing, 1992) that the problem of Doppler imaging can be fully linearized when the *shape* of the local spectrum does not depend on the position on a stellar surface (while allowing the local continuum intensities to vary). Under this assumption the

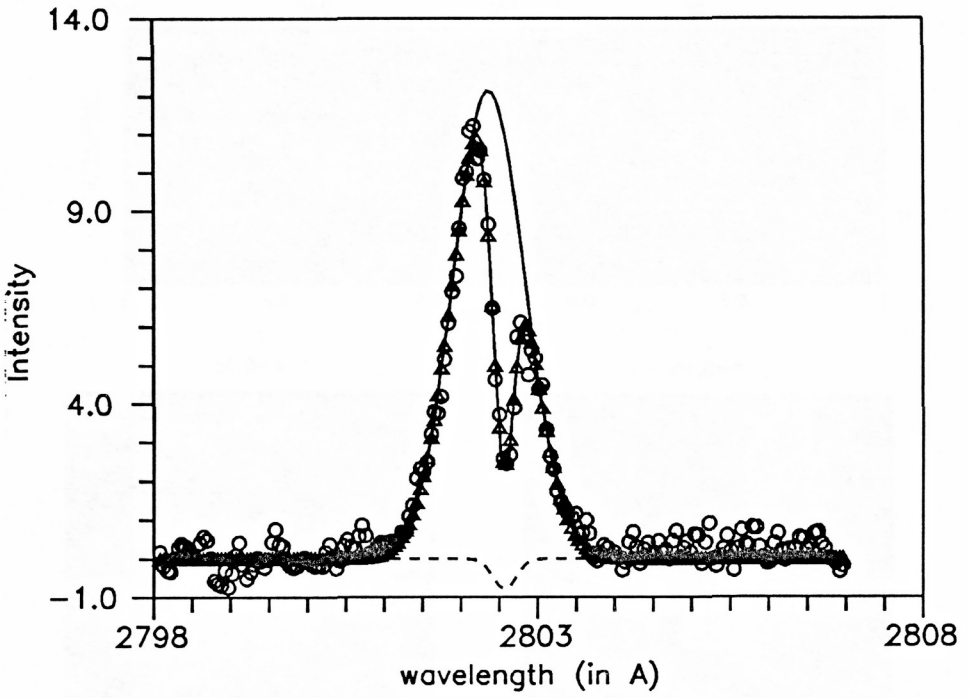

Fig. 1. The observed (circles), the best fitted (full line with triangles), the reconstructed emission (full line) and absorption (dashed line) spectral line profiles.

problem can be translated into the indirect imaging terms by considering the image-data transformation in the linear form :

$$Y_i = \sum_{j=1}^{J} R_{ij} X_j \qquad i = \overline{1, I}.$$

where the vector Y_i represents the data, the matrix R is a mapping, which takes a function in the image space into a function in the data space and X_j is the image vector. This representation, ensuring the uniqueness of the solution, leads also to significant computational savings.

Since the inverse matrix R^{-1} is badly conditioned a solution is obtained by minimizing an appropriate "regularising functional", of the image function subject to the classical constraint $\chi^2 = \chi_0^2$:

$$\sum_{i=1}^{I} \left((Y_i - \sum_{j=1}^{J} R_{ij} \hat{X}_j)/\sigma_i \right)^2 = \chi_0^2,$$

where χ_0^2 is determined by the required confidence level to data statistics χ^2, $\hat{X}_J$ is the solution, and σ_i is the standard error in the datum i. The data statistic χ^2 is

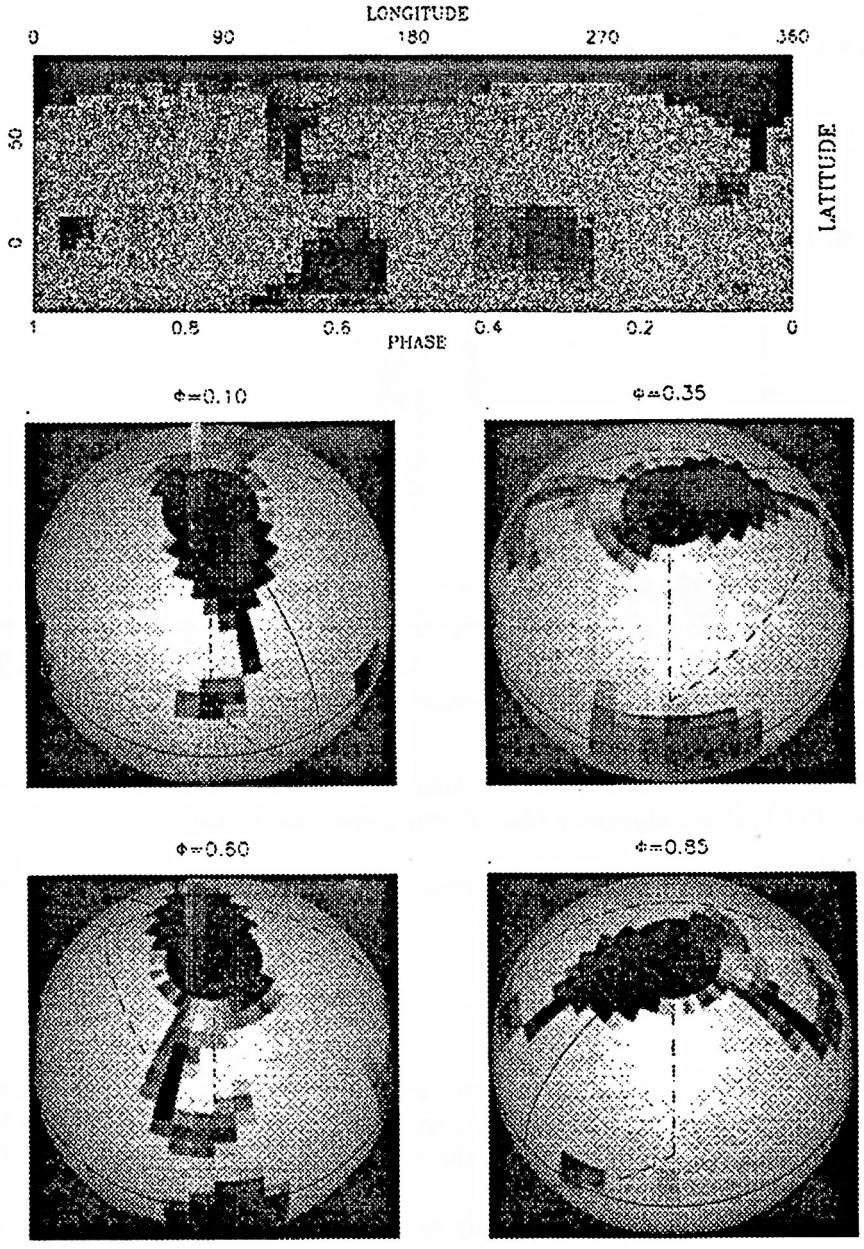

Fig. 2. The reconstructed image of HR 1099.

used to measure the discrepancy between the observed and modeled data, while the χ^2 surfaces are convex ellipsoids in J dimensional image space.

The search strategy employed for the image reconstruction consisted in minimizing χ^2 until reaching the hypersurface χ_0^2 by the constrained gradient method. The entropy is further maximized on the hypersurface $\chi^2 = \chi_0^2$ until reaching the parallelity

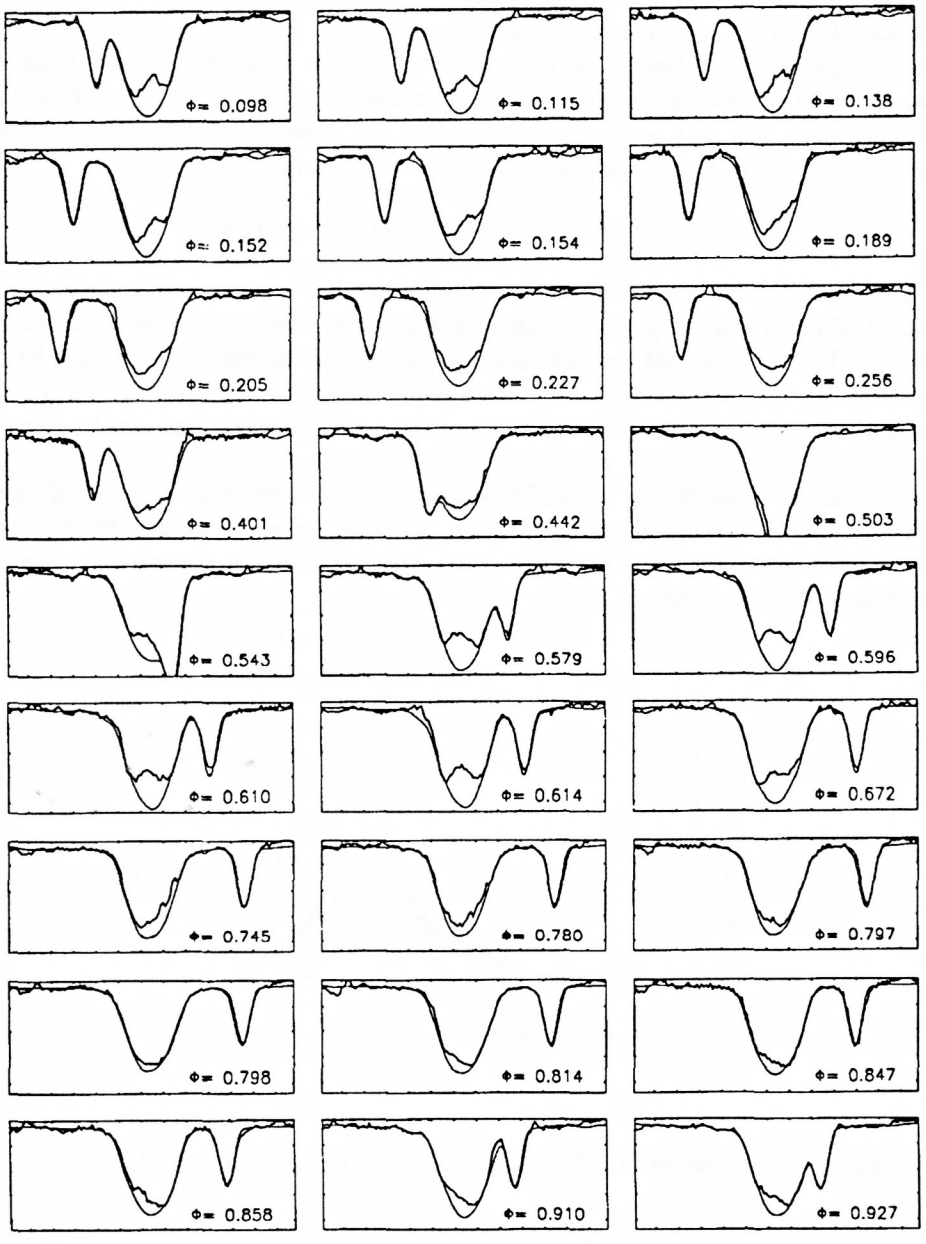

Fig. 3. The observed line profiles.

of the gradients of χ^2 and entropy, i.e., practically, until reaching the neighbourhood of the maximum entropy point defined so that the cosine of the angle between the gradients is greater than or equal to 0.99.

An example the image reconstruction of the RS CVn binary system HR 1099 is shown in Fig. 2, based on a set of high-resolution and high signal-to-noise ratio spectra (Fig. 3). The maps show cool ($T = 2500K$) extended spotted structures : one at high latitude adjacent to the rotation pole and symmetric versus longitude, two nearly equatorial spots positioned approximately symmetrically with respect to the secondary star and several smaller spots. The presence of bright photospheric faculae seems to be established slightly above the detection level.

4. THE CASE OF AGN'S LINES

The spectral lines of active galactic nuclei (AGN), i.e., quasars and Seyfert galaxies, consist of parts that originate in different regions around the nucleus. The models propose that the observed line is formed usually in two regions : Broad Line Region and Narrow Line Region (see, e.g., Nazarova, 1991). For determining the physical conditions in these regions we have to reconstruct their spectral line profiles from the observed one.

Here, as an example, we show the result of a fit of observed L_α spectral line of MKN 335 Syfert galaxy with five gaussian functions using the inverse method (Fig. 4). The emission part of the Lα line is fitted with two, and the absorptions ones with three gaussian functions.

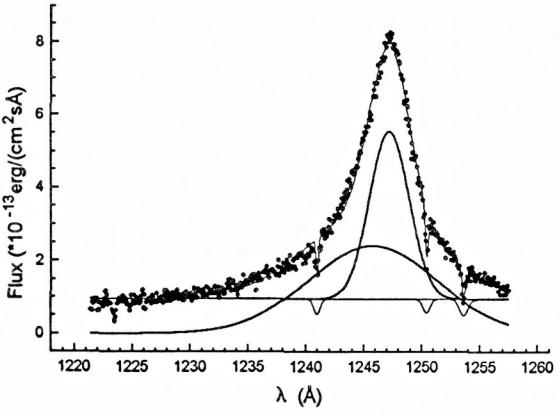

Fig. 4. The observed L_α line profile (dots) and its Gaussian fit (full line).

References

Jankov, S. : 1992, Ph.D. thesis, Paris VII, Paris
Jankov, S., Foing, B.H. : 1992, *Astron. Astrophys.* **256**, 533-550.
Nazarova L. S., 1991, *Sops. Spec. Astrophys. Obs.* **66**, 37.